INTERNATIONAL JOURNAL OF APPLIED TECHNOLOGY RESEARCH
2022, VOL. 3, NO. 2, pp. 135-148
https://ijatr.polban.ac.id/

POLBAN

Optimization of Device Installations in the Home Solar Power Generation System

[a]Sri Paryanto Mursid, [a]Ignatius R Mardiyanto*, [a]Sri Utami

[a]Energy Engineering Department, Politeknik Negeri Bandung, Bandung 40559, Indonesia

Received April 8, 2022; Revised April 21, 2022; Accepted June 13, 2022; Published October 1, 2022

ABSTRACT

One of the main challenges in building a Solar Power Generation System at home or a Home Solar Power Plant (Home SPP) is choosing component specifications according to price. The main components of Home SPP are photovoltaic (PV) panels, inverters, and wiring systems. Given the strict price constraints, the selection of parts available on the commercial market is generally of low quality. However, low-quality components can still provide a significant advantage by optimizing the plant design. This research proves that the proper configuration can reduce electricity bills by 52.2%. This configuration does by choosing a Grid Tie Inverter (GTI) with a high working voltage and a 12 Volt PV configured in a parallel series circuit to work at 24 Volts. In addition, the 12 Volt PV panels configured in series to 24 Volts are proven to increase the conversion efficiency.

KEYWORDS

Optimization Device Installation
Home Solar Power
Grid Tie Inverter
Proper DC Configuration

INTRODUCTION

Home solar power plants (SPP) are increasingly easy to find nowadays. Some families who care about green earth have started using their houses' roofs to generate electricity. The main advantage of solar power generation is that there is no need to buy solar energy sources.

In Indonesia, where the equator crosses, solar energy can obtain abundantly for free. However, it needs solar panels to power daily household activities on the roof. The concept is cheap and straightforward; the challenge is to make a reliable PV installation using a commercially available device in the market with relatively cheap and low quality.

LITERATURE REVIEW

The rapid increase in PV energy use is related to solar cells' increasing efficiency and manufacturing of solar panels [1]–[3]. The PV generators can either be grid-connected (operate in distributed generation systems) or can work in stand-alone (autonomous) systems [4]–[6]. Both types result in the need for knowledge in choosing the type of solar panel and the financial problems that accompany it [7]. Furthermore, a control system that can be used in solar power

*Corresponding Author: ignatius.mardiyanto@polban.ac.id

generation applications is also needed [8]–[11], integration into conventional [12]–[15] or with another renewable generation [7], [16]–[23], synchronization [24], optimization [25]–[34].

Home SPP installation has unique problems that do not always encounter Solar Power Generation experiments in the laboratory. For example, the limited choice of PV placement strictly depends on the available empty area [6], [35], [36]. The finished house's architecture and construction never be overhauled to install Home SPP. Also, funding is the main obstacle in the installation of Home SPP. The selection of home SPP components is a critical step, strongly influenced by the available funds, which are often minimal. Device selection becomes even more challenging when the choice is for products sold with specification data polished according to marketing conventions. The question is, how reliable is this marketing data, and how to prove it? This research experiments to install Home SPP with some of the market's equipment and get the optimum configuration.

RESEARCH METHOD

This study uses a work sequence or a research method to apply the home SPP system optimum design. The first step is to choose components that are on the commercial market. Next, make the optimal Home SPP configuration design based on existing data. Finally, the design results are installed in the home electrical system that has been connected to the State Electricity Company (PLN). Next, design simulation, observation, and measurement are conducted to obtain data and see the Home SPP system's behaviors. Finally, data processing and analysis are carried out to assess and conclude the performance of Home SPP.

Home SPP Configuration

Home SPP Installation can use DC (direct current) or AC (alternating current) configurations [1]. DC voltage is a natural characteristic of a PV panel composed of a series of photovoltaic cells using PN Junction as its basic component. A PN Junction exposed to photons produces a direct electric current from semiconductor P to N [ref]. So that SPP is a DC electric energy generator and can be directly used by DC loads such as LED bulbs. Meanwhile, an inverter must convert a DC to AC voltage [13].

Solar Power Plant Installation

This research is based on observational data on the Home SPP Installation, deliberately installed at home. Its configuration allows it to be changed both on-grid and off-grid. It is also possible to change the type and specification of the inverter (GTI in this case) as one of its main components. The solar panel installations are divided into two array groups to support configuration flexibility during the research. The PV array configuration diagram shows in Figure 1. There are ten (10) panels with PV specifications as follows.

Table 1. PV Panel Specification Data

Rated Maximum Power (Pm)	:	100W
Tolerance	:	+/-3%
Voltage at Pmax (Vmp)	:	17.8V
Current at Pmax (Imp)	:	5.62A
Open-Circuit Voltage (Voc)	:	21.8V
Short-Circuit Current (Isc)	:	6.05A
Normal Operating Cell Temp (NOCT)	:	47±2 °C
Maximum System Voltage	:	1000VDC
Operating Temperature	:	-40 °C to +85 °C
Cell Technology	:	Mono-crystal
Dimension(mm3)	:	1030x670x 30

The table of the PV Specification Data set does not mention efficiency. However, it can easily be calculated because there is information on the dimensions, namely 1030x670x30 with Rated Maximum Power (P_m): 100W. While the maximum normal surface irradiance (I_p) is approximately 1000 W/m2 at sea level on a clear day [4]. If the area of PV (A_{PV}) is 1030 (length) x 670 (width) = 0.6901 m2. So, the efficiency of PV (η_{PV}) can be calculated by equation (1).

$$\eta_{PV} = \left(\frac{\left({}^{P_m}/_{A_{PV}} \right)}{I_p} \right) \times 100\% \quad (1)$$

The PV efficiency is obtained by entering the appropriate specification data in equation (1). The results of calculating the efficiency are described in this section.

$$\eta_{PV} = \left(\frac{\left({}^{100}/_{0.6901} \right)}{1000} \right) \times 100\% = 14.49\%$$

This efficiency value is a claim (calculated based on their data) from the PV manufacturers in their laboratory test results. This research proves whether this value is actually in actual conditions in the field.

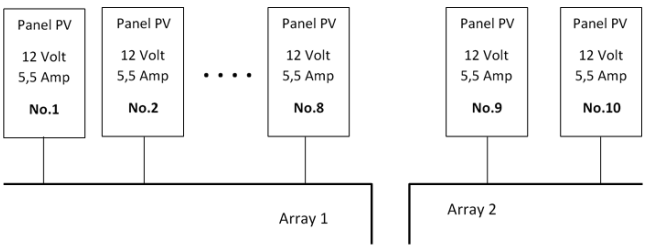

Figure 1. Two-path array arrangement

Array 1 consists of 8 PV panels with a total theoretical installed power of 800 Watts. And then, array 2 consists of 2 PV panels with 200 Watts of power. Each Array allows us to arrange in parallel and serial configurations. The parallel structure makes it possible to get a higher working voltage, for example, 24 Volts. The current flowing into the load becomes smaller with constant power—a smaller electric current provides an advantage in choosing a shorter conductor cable at a lower price.

Table 2. Grid Tie Inverter Specification Data

GTI1	GTI2
Rated Power 1000W	Rated Power: 600W
Compatible with Solar Panels 60 cells/24V,	Compatible with Solar Panels: 43 cells/12V
Vmp: 26-30V,	DC Input Range: 11-32V_{DC}
Voc: 34-38V;	MPPT Voltage: 15-22V_{DC}
72 cells/36V,	DC MAX. Current: 38A
Vmp: 35-39V,	AC Output : 230VAC (190-260V_{AC})
Voc: 42-46V_{DC}	Frequency: 50Hz/60Hz (Auto control)
Input Range 20-45V	Power Factor: >98%
MPPT Voltage 28-36 V_{DC}	THD: 5 %
DC MAX. Current 60A	Phase Shift: 2 %
AC Output 230VAC (190-260V_{AC})	Peak Efficiency: 86 %
Frequency 50Hz/60Hz(Auto control)	Stable Efficiency: 88 %
Power Factor > 97.5%	Protection: Islanding; Short-circuit; Low
THD 5 %	Voltage;
Phase Shift 2 %	Over Voltage; Over temperature Protection
Efficiency 230VAC(190-260V_{AC})	Working Temperature: -20°C-65°C
Peak Efficiency 87%	
Stable Efficiency 85%	
Operating Temperature -20 °C-45 °C	

The next main component is the Grid Tie Inverter (GTI). Again, two GTIs with different specifications were selected, the GTI1 had a working voltage of 24 Volts, and the GTI2 had an operating voltage of 12 Volts. GTI1 is used to experiment with PV panels in parallel configurations, while GTI2 is used when PV panels configure in series. The specifications of the two GTIs are shown in Table 2.

The Home SPP system in this study is also equipped with energy storage devices in the form of Valve Regulated Lead Acid (VRLA) dry batteries, BCC (battery charge controller), Pulse Width Modulation (PWM), and Maximum Power Point Tracking (MPPT) as well as a 1500 Watt pure sinusoidal inverter. This additional device is used for backup power when the grid of PLN goes out or off-grid. Also, for further experiments in the future.

The Home SPP system's main control board includes GTI, Pure Sine Inverter, BCC, MCB, and meter equipment at each important measuring point. This meter equipment makes it possible to know voltage (Volts), current (Ampere), power (Watts), energy (kWH), frequency, and Cos Phi. The basic configuration of the Main Control Board diagram shows in Figure 2.

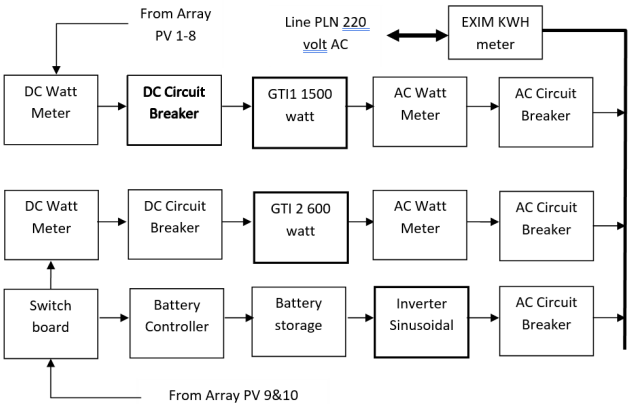

Figure 2. Main control board diagram

The installed equipment is a commercial product on the market. However, this research does not discuss the brand but determines how the product specifications match the test results.

Exploring the Characteristics of PV Panels

The photovoltaic cell has an equivalent circuit, shown in Figure 3, consisting of an Iph current, a diode with current Io, shunt resistor Rs, and parallel resistor Rp [rev]. Overall, a single PV panel also behaves like a one-cell equivalent circuit.

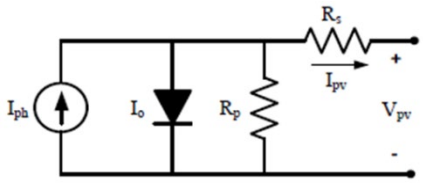

Figure 3. Solar cell equivalent circuit

Figure 3 shows that PV current is proportional to $I_{pv} = I_{ph} - I_o\{f(R_p, R_s, V_{pv}, q, N, A, K, T, G)\}$. Where: q is the electron charge constant, N is the number of cells in a PV panel, A is the ideal diode factor, K Boltzmann constant, T temperature, and G are solar irradiance received by solar cells [14]. The complete equation of IPV shows in formula (2).

$$I_{pva} = I_{ph} - I_{o1} \times \left[\exp\left(\frac{q(V_{pv} + I_{pv}R_s)}{N_s AKT_k}\right) - 1\right] - \frac{(V_{pv} + I_{pv}R_s N_s)}{R_p N_s} = 0 \qquad (2)$$

PV panels have a maximum Ipv when their output is short-circuiting ($V_{pv} = 0$ Volts). Conversely, when the output power is open ($I_{pv} = 0$), the Vpv is maximum. So, the PV panel produces an output power that changes with changes in load. There is a point where multiplying IPV by V_{pv} makes full power (P_{pv}), known as Maximum Power Point (MPP). The simulation uses the PV Module software for mobile devices downloaded from the Google Play store. Simulation graph results are used for the rest of this paper.

Maximum Power Point (MPP) occurs at a voltage of 15 Volts and a current of 8 Amps. The Maximum Power-Point position is at graph IV's knee and constantly changes depending on the sun's radiation and load.

PV Performance Simulation

This simulation aims to prove whether the "commercial" specifications of PV are used, see Table 1, and correspond to the results of calculations using Equation 2. The simulation uses the PV Module software, whereas the computation method uses Equation 2 [17]. Therefore, the first step in the simulation is to enter data from the PV specification in Table 1 into the PV Module Program data input screen. The results can see in Figure 4 a. then, by pressing the Calculation button, the calculation results for the outcome variable were obtained, as shown in Figure 4b.

(a) (b)

Figure 4. (a) PV variable, (b) Calculation result

Furthermore, the PV Module Program simulates and plots the calculation results graphs I to V, P to V for Irradiant 1000 W/m2, 600 W/m2, and 300 W/m2 at 250 o C and 450 C.

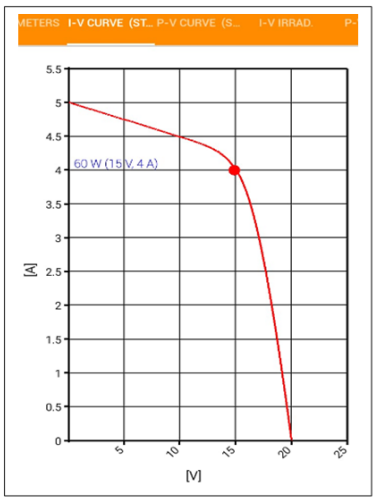

Figure 5. Plotting I to V

The curve in Figure 5 shows that the MPP occurs at the coordinate point (V, I) = (15.4). With the simple power equation P = VI, the maximum P_{PVmax} power obtained from this commercial PV is 60 Watts. So, the PV efficiency from the simulation results using Equation 3 is

$$\eta_{riel} = \left(\frac{P_{PVmax}}{I_p}\right) \times 100\% \quad (3)$$

$$\eta_{riel} = \left(\frac{60}{1000}\right) \times 100\% = 6\%.$$

While the calculation of efficiency (ηPV) from the PV data quotation obtained ηPV = 14.49%. So, the efficiency of the simulation results is only 0.41 of the efficiency based on these commercial data. Therefore, it is never possible to get the PV power output installed in subsequent installations, producing 100 Watts of power, as stated in the PV packaging data.

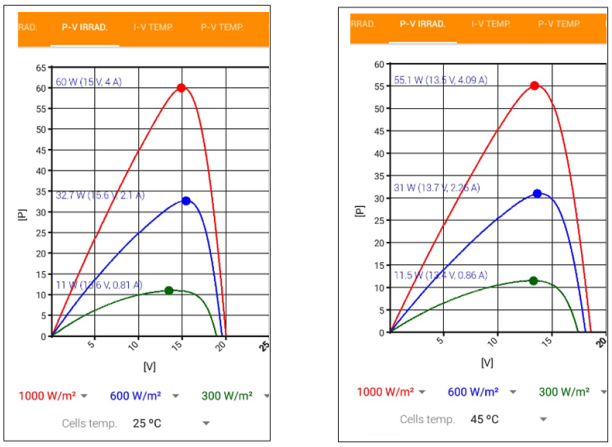

Figure 6. Results of plotting p to v with changing irradiation and temperature

The panel surface temperature affects solar energy conversion to electrical energy by PN Junction in PV cells. Figure 6 shows that MPP = 60 Watts occurs when solar irradiation Ip is 1000 W/m2 at a panel surface temperature of 25 °C. When operating in the sun, the Temperature of the solar panels rises to 45 °C. In the plot to the right of Figure 6b, it can see that the MPP drops to 55.1 Watts at Ip 1000 W/m2 with a panel surface temperature of 250C.

The production of electric power from solar radiation energy conversion by this limited PV is also getting smaller due to the wiring system's conductor [ref]. Weather is also very influential, especially the potential for clouds to cover sunlight.

Partial closure of the PV panel array by the shadows of buildings or trees also dramatically affects the Home SPP's overall performance [23].

This study seeks to take advantage of these limited conditions by selecting the most optimum configuration. So, it can obtain a Home SPP capable of producing maximum power with market-quality commercial equipment.

DISCUSSION

The experiment's equipment comprises the Solar power meter, Lux meter, digital thermometer, and several multimeters, including measuring voltage, current, power, energy, frequency, and cos-phi. These measuring instruments are attached to the main control board as a monitor device. This research does not require a high-precision measuring tool but rather consistency in its measurement.

The first experiment was to measure the characteristics of the PV panel to obtain actual data. Then, the results can compare with manufacturer-supplied PV specification data. The binary load is used during the experiment. The connected loads are marked with a switch number. After that, experiments are carried out repeatedly to obtain a series of data that can be processed. After the data is collected, each measured variable's consistency can be seen. In this discussion, data samples are taken to show the performance of PV Table 3 provides an example of the data from the time at 11:45 measurement. During the day, the Solar Power Meter shows 973 Watts/m2, and the measured PV surface temperature is 47.2 °C. Furthermore, the graph of PV voltage versus power can see in Figure 7.

Table 3. Measurement data from PV Home system

V (volt)	I (Amp)	P(Watt)	P/10	Load step
19.9	0	0	0	0.0.0.0.0
19.6	0.57	11.172	1.1172	1.0.0.0.0
18.1	2.87	51.947	5.1947	0.2.0.0.0
17.7	3.36	59.472	5.9472	1.2.0.0.0
13.6	4.85	65.96	6.596	0.2.3.0.0
11.5	4.85	55.775	5.5775	1.2.3.0.0
7.2	4.86	34.992	3.4992	0.2.3.4.0
6.42	4.87	31.2654	3.1265	1.2.3.4.0
0.2	4.89	0.978	0.0978	1.2.3.4.5

Temp °C	Lux x 1000	SPM Watt/m²
47.2	843	973

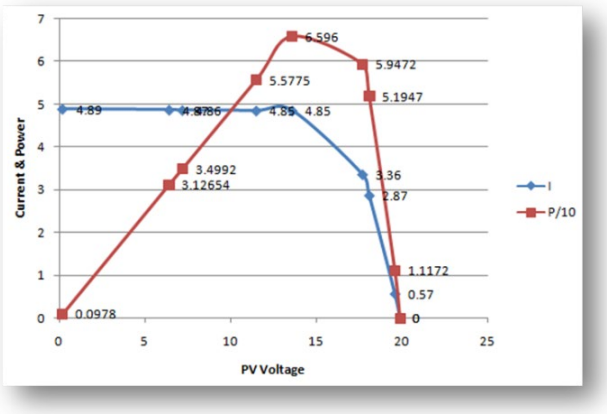

Figure 7. Graph of PV plotting I-V and PV Measurement

It is interesting to note that these measurement results indicate an MPP condition with a value of 65.96 watts. This rated PV output power exceeds the simulation results showing an amount of 60 Watts. This difference can cause by faulty measuring equipment, inaccurate factory specification data that affects the final simulation results, or inconsistencies in the PV product itself. However, the difference is less pronounced and remains below the 100 Watts claimed by the manufacturer. Therefore, it does not change the quality level of this commercial PV product. Likewise, the efficiency value of the measured PV is

$$\eta_m = \left(\frac{P_m}{SPM}\right) \times 100\% \quad (4)$$

$$\eta_m = \left(\frac{65.67}{973}\right) \times 100\% = 6.78\%$$

This measurement result's efficiency value is higher than the simulation result's efficiency (6%). However, it is still far from the manufacturer's claim. However, it should still be appreciated as a positive value.

With low quality and efficiency conditions, every watt of energy produced by PV is precious. Therefore, it must utilize and reduce the losses of conductors and GTI (grid-tie inverter).

Conductor losses can reduce by choosing high-quality cables. However, this solution is another disadvantage because of the very high price. Therefore, the answer is to increase the voltage, resulting in less current passing through the conductor. So that cheaper conductors can deliver the same amount of electric power.

The selection of the GTI also plays an important role. The assumption is that the smaller the current is, the easier it is to get a higher conversion efficiency for the same power. Therefore, choosing a GTI with a higher operating voltage is necessary. There are many GTIs with various operating voltages on the market. However, this experiment only compares the 12 Volt GTI with the GTI 24 Volt.

The experiment uses a PV circuit and its equipment, as shown in the diagram in Figure 2. The total PV used is ten panels, with panels 1 to 8 installed in parallel series. That is (1 with 2, 3 with 4, 5 with 6, 7 with 8, then the series pairs are parallel) with a working voltage of 24 Volts to form Array 1. While panels 9 and 10 are parallel to remain at a working voltage of 12 Volts to form Array 2. So that the area of AArray(1) = 5.52 m2 andAArray (2) = 1.38 m2.

A snapshot of the measurement results is shown in Table 4 below.

Table 4. Measurement results for comparison array 1 and array 2

No.	A clock's	Temp (°C)	SPM (Watt/m^2)	Lux x 1000	GTI 1 (Watt)		GT2 (Watt)	
					In	Out	In	Out
1	9:42	45.9	800	725	360	331	86.60	72.20
2	9:51	45.6	1035	890	442	386	91.00	75.30
3	10:00	46.3	1075	924	460	409	91.20	75.80
4	10:10	45.9	1000	890	430	385	88.90	73.11
5	10:20	45.6	900	789	401	360	84.01	68.80

No.	A clock's	Temp (°C)	SPM (Watt/m²)	Lux x 1000	GTI 1 (Watt)		GT2 (Watt)	
					In	Out	In	Out
6	10:30	45.1	992	863	440	394	88.20	72.20
7	10:40	45.6	980	846	419	372	89.00	72.80
8	10:45	47.6	1016	880	445	395	88.10	73.80
9	10:55	48.1	1046	905	431	380	89.00	73.30
10	11:00	45.5	1046	905	449	389	89.70	74.30
11	11:10	45	1052	912	455	403	90.00	74.00

The input of the GTI 1 is the output power produced from PV panels 1 - 8 with a maximum output according to the factory specification data of 800 Watts at 24 Volts. While the GTI 2 is input from PV panels 1 and 2 with a power of 200 Watts/12 Volts.

The conversion efficiency of the GTI defines as the output power divided by the input power. Therefore, the efficiency of GTI 1 and GTI 2 can be found by calculating the existing data with this efficiency definition. At the same time, the following equation can calculate the Array's efficiency below.

$$\eta_{\text{Array}} = \left(\frac{P_{inGTI}}{P_{\text{Array}}}\right) \times 100\% \tag{5}$$

While the following equation can calculate PArray

$$P_{\text{Array}} = \eta_{\text{Array}} \times A_{\text{Array}} \times Iradiation_{SPM} \tag{6}$$

Using Equations 4 and 5, the efficiency of Array1, Array2, GTI 1, and GTI 2 is obtained, as shown in Table 5.

Table 5. The efficiency of PV and GTI arrays

No	η_{Array1}	η_{Array2}	η_{GTI1}	η_{GTI2}
1	56.25	54.13	91.94	83.37
2	53.38	43.96	87.33	82.75
3	53.49	42.42	88.91	83.11
4	53.75	44.45	89.53	82.24
5	55.69	46.67	89.78	81.90
6	55.44	44.46	89.55	81.86
7	53.44	45.41	88.78	81.80
8	54.75	43.36	88.76	83.77
9	51.51	42.54	88.17	82.36
10	53.66	42.88	86.64	82.83
11	54.06	42.78	88.57	82.22

The values are listed in Table 5, shown by comparing the efficiency of Array 1 and Array 2 and the GTI 1 and GTI2. They clarified the difference, and the data in the table is plotted in a graph.

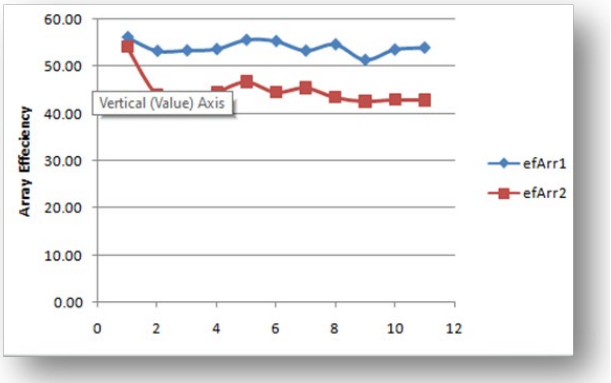

Figure 8. Comparison chart of array efficiency

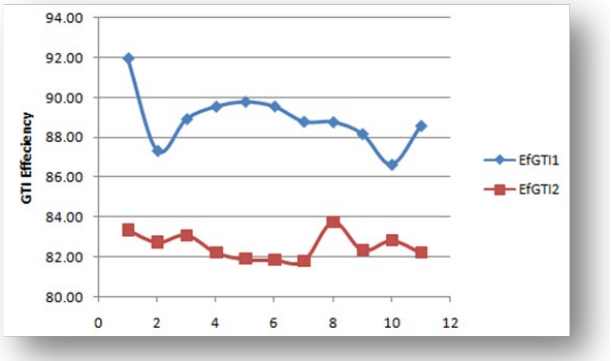

Figure 9. Comparison graph of GTI efficiency

Figure 8. It shows that Array 1, with an operating voltage of 24 Volts, the sum of the two PVs' voltages connected in series, shows higher efficiency than Array 2, with an operating voltage of 12 Volts.

Likewise, GTI 1, with an operating voltage of 24 Volts, shows a higher conversion efficiency than GTI2, with 12 Volts, as shown in Figure 9.

Since July, experiments have been conducted. The GTI began to connect to the PLN grid in August. Comparing the June, July, and October bills shows this Home SPP's economic effect. Accounts for August and September do not include experiments because experiments are carried out by making configuration changes, so the data was less convincing. The bill comparison shows in Figure 10.

CONCLUSION

This study proves that the equipment for building Home SPP, obtained in the low-mid-level commercial market tends to have a lower efficiency than the specification data included in the product. Therefore, carefully selecting Home SPP components in the retail market is necessary. In addition, it would be wise to compare testimonials from other consumers.

A mini-grid system with a PV energy source increases the system's operating voltage. This efficiency increase applies to solar cells made with medium to low-quality materials. Thus, a low-

quality PV serial connection to raise the voltage to match the inverter operating voltage improves performance.

Economically, Home SPP builds benefits carefully by lowering monthly electricity bills. However, we must also follow the legal law of power export-import regulations to do this.

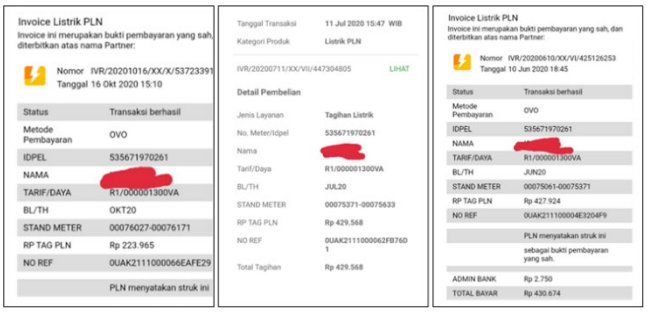

Figure 10. Electricity Bill for October, July, and June 2020

The bill in June was IDR 427,924.00, and in July, it was IDR 429,568. Although not shown, August and September bills tend to fall. However, a significant decline appeared in October, namely IDR. 223,965.00. This bill reduction was around 52%.

ACKNOWLEDGEMENTS

Thank you to the Bandung State Polytechnic for funding this research.

REFERENCES

[1] S. K. Sahoo, "Renewable and sustainable energy reviews solar photovoltaic energy progress in India: A review," *Renew. Sustain. Energy Rev.*, vol. 59, pp. 927–939, 2016, doi: 10.1016/j.rser.2016.01.049.

[2] "Diffuse Sky Radiation," in *Van Nostrand's Scientific Encyclopedia*, 2005. doi: 10.1002/0471743984.vse2550.

[3] T. J. Rossi, J. F. Escobedo, C. M. dos Santos, L. R. Rossi, M. B. P. da Silva, and E. Dal Pai, "Global, diffuse and direct solar radiation of the infrared spectrum in Botucatu / SP / Brazil," *Renew. Sustain. Energy Rev.*, vol. 82, pp. 448–459, 2018, doi: 10.1016/j.rser.2017.09.030.

[4] L. Tianze, L. Hengwei, J. Chuan, H. Luan, and Z. Xia, "Application and design of solar photovoltaic system," *J. Phys. Conf. Ser.*, vol. 276, no. 1, 2011, doi: 10.1088/1742-6596/276/1/012175.

[5] J. T. Bialasiewicz, "Renewable energy systems with photovoltaic power generators: Operation and modeling," *IEEE Trans. Ind. Electron.*, vol. 55, no. 7, pp. 2752–2758, 2008, doi: 10.1109/TIE.2008.920583.

[6] M. Bajaj and A. K. Singh, "An analytic hierarchy process-based novel approach for benchmarking the power quality performance of grid-integrated renewable energy systems," *Electr. Eng.*, vol. 102, no. 3, pp. 1153–1173, 2020, doi: 10.1007/s00202-020-00938-3.

[7] R. Du and P. Robertson, "Cost-Effective Grid-Connected Inverter for a Micro Combined Heat and Power System," *IEEE Trans. Ind. Electron.*, vol. 64, no. 7, pp. 5360–5367, 2017, doi: 10.1109/TIE.2017.2677340.

[8] N. Femia, D. Granozio, G. Petrone, G. Spagnuolo, and M. Vitelli, "Optimized one-cycle control

in photovoltaic grid connected applications," *IEEE Trans. Aerosp. Electron. Syst.*, vol. 42, no. 3, pp. 954–971, 2006, doi: 10.1109/TAES.2006.248205.

[9] M.S. Mahmodian, R. Rahmani, E.Taslimi, and S. Mekhilef., "Step By Step Analyzing, Modeling and Simulation of Single and Double Array PV system in Different Environmental Variability," in *2012 International Conference on Future Environment and Energy IPCBEE*, 2012, vol. 28. [Online]. Available: www.ipcbee.com/vol28/8-ICFEE2012-F016.pdf

[10] I. Abadlia, L. Hassaine, A. Beddar, F. Abdoune, and M. R. Bengourina, "Adaptive fuzzy control with an optimization by using genetic algorithms for grid connected a hybrid photovoltaic–hydrogen generation system," *Int. J. Hydrogen Energy*, vol. 45, no. 43, pp. 22589–22599, 2020, doi: 10.1016/j.ijhydene.2020.06.168.

[11] M. Stojcic, A. Stjepanovic, and D. Stjepanovic, "Anfis model for the prediction of generated electricity of photovoltaic modules," *Decis. Mak. Appl. Manag. Eng.*, vol. 2, no. 1, pp. 35–48, 2019, doi: 10.31181/dmame1901035s.

[12] S. Aittahar, V. François-Lavet, S. Lodeweyckx, D. Ernst, and R. Fonteneau, *Imitative learning for online planning in microgrids*, vol. 9518. 2015. doi: 10.1007/978-3-319-27430-0_1.

[13] J. F. Ardashir, M. Sabahi, S. H. Hosseini, F. Blaabjerg, E. Babaei, and G. B. Gharehpetian, "A Single-Phase Transformerless Inverter with Charge Pump Circuit Concept for Grid-Tied PV Applications," *IEEE Trans. Ind. Electron.*, vol. 64, no. 7, pp. 5403–5415, 2017, doi: 10.1109/TIE.2016.2645162.

[14] O. Ezinwanne, F. Zhongwen, and L. Zhijun, "Energy Performance and Cost Comparison of MPPT Techniques for Photovoltaics and other Applications," *Energy Procedia*, vol. 107, pp. 297–303, 2017, doi: 10.1016/j.egypro.2016.12.156.

[15] T. Shimizu, O. Hashimoto, and G. Kimura, "A novel high-performance utility-interactive photovoltaic inverter system," *IEEE Trans. Power Electron.*, vol. 18, no. 2, pp. 704–711, 2003, doi: 10.1109/TPEL.2003.809375.

[16] N. Kelly, M. Sasso, G. Angrisani, and C. Roselli, "Impact of microgeneration systems on the low-voltage electricity grid," 2014.

[17] S. Talari, M. Yazdaninejad, and M. R. Haghifam, "Stochastic-based scheduling of the microgrid operation including wind turbines, photovoltaic cells, energy storages and responsive loads," *IET Gener. Transm. Distrib.*, vol. 9, no. 12, pp. 1498–1509, 2015, doi: 10.1049/iet-gtd.2014.0040.

[18] S. Silvestre, A. Boronat, and A. Chouder, "Study of bypass diodes configuration on PV modules," *Appl. Energy*, vol. 86, no. 9, pp. 1632–1640, 2009, doi: 10.1016/j.apenergy.2009.01.020.

[19] I. J. Hasan, N. A. J. Salih, and N. I. Abdulkhaleq, "Three-phase photovoltaic grid inverter system design based on PIC24FJ256GB110 for distributed generation," *Int. J. Power Electron. Drive Syst.*, vol. 10, no. 3, pp. 1215–1222, 2019, doi: 10.11591/ijpeds.v10.i3.1215-1222.

[20] S. H. Nengroo *et al.*, "An optimized methodology for a hybrid photo-voltaic and energy storage system connected to a low-voltage grid," *Electron.*, vol. 8, no. 2, 2019, doi: 10.3390/electronics8020176.

[21] H. Ibrahim and N. Anani, "Study of the effect of different configurations of bypass diodes on the performance of a PV string," *Smart Innov. Syst. Technol.*, vol. 163, pp. 593–600, 2020, doi: 10.1007/978-981-32-9868-2_50.

[22] F. F. Ahmad, C. Ghenai, A. K. Hamid, and M. Bettayeb, "Application of sliding mode control for maximum power point tracking of solar photovoltaic systems: A comprehensive review," *Annu. Rev. Control*, vol. 49, pp. 173–196, 2020, doi: 10.1016/j.arcontrol.2020.04.011.

[23] A. Ali *et al.*, "Review of online and soft computing maximum power point tracking techniques under non-uniform solar irradiation conditions," *Energies*, vol. 13, no. 12, 2020, doi:

10.3390/en13123256.

[24] F. Shahnia and S. Bourbour, "A practical and intelligent technique for coupling multiple neighboring microgrids at the synchronization stage," *Sustain. Energy, Grids Networks*, vol. 11, pp. 13–25, 2017, doi: 10.1016/j.segan.2017.06.002.

[25] M. Seyedmahmoudian, A. Mohamadi, S. Kumary, A. M. T. Oo, and A. Stojcevski, "A Comparative Study on Procedure and State of the Art of Conventional Maximum Power Point Tracking Techniques for Photovoltaic System," *Int. J. Comput. Electr. Eng.*, vol. 6, no. 5, pp. 402–414, 2014, doi: 10.17706/ijcee.2014.v6.859.

[26] L. L. Jiang, R. Srivatsan, and D. L. Maskell, "Computational intelligence techniques for maximum power point tracking in PV systems: A review," *Renew. Sustain. Energy Rev.*, vol. 85, pp. 14–45, 2018, doi: 10.1016/j.rser.2018.01.006.

[27] A. N. A. Ali, M. H. Saied, M. Z. Mostafa, and T. M. Abdel- Moneim, "A survey of maximum PPT techniques of PV systems," *2012 IEEE Energytech, Energytech 2012*, 2012, doi: 10.1109/EnergyTech.2012.6304652.

[28] M. Seyedmahmoudian, B. Horan, R. Rahmani, A. M. T. Oo, and A. Stojcevski, "Efficient photovoltaic system maximum power point tracking using a new technique," *Energies*, vol. 9, no. 3, 2016, doi: 10.3390/en9030147.

[29] R. Faranda and S. Leva, "Energy comparison of MPPT techniques for PV Systems," *WSEAS Trans. power Syst.*, vol. 3, no. 6, pp. 446–455, 2008, [Online]. Available: http://www.wseas.us/e-library/transactions/power/2008/27-545.pdf

[30] M. Tung, D. Aiguo, P. Hu, and D. Nirmal, "Evaluation of microcontroller based maximum power point tracking methods using dSPACE platform," 2006.

[31] M. Bodur and M. Ermis, "Maximum power point tracking for low power photovoltaic solar panels," in *Mediterranean Electrotechnical Conference - MELECON*, 1994, vol. 2. doi: 10.1109/melcon.1994.380992.

[32] R. F. Coelho, F. M. Concer, and D. C. Martins, "A MPPT approach based on temperature measurements applied in PV systems," 2010. doi: 10.1109/INDUSCON.2010.5740006.

[33] G. Wibisono, S. Pramono, and M. Muslim, "MPPT Menggunakan Metode Hibrid JST Dan Algoritma Genetika Untuk Sistem Photovoltaic," *J. EECCIS*, vol. 8, no. 2, pp. 181–186, 2014.

[34] M. Bahrami *et al.*, "Hybrid maximum power point tracking algorithm with improved dynamic performance," *Renew. Energy*, vol. 130, pp. 982–991, 2019, doi: 10.1016/j.renene.2018.07.020.

[35] N. Golovanov, G. C. Lazaroiu, M. Roscia, and D. Zaninelli, "Power quality assessment in small scale renewable energy sources supplying distribution systems," *Energies*, vol. 6, no. 2, pp. 634–645, 2013, doi: 10.3390/en6020634.

[36] V. François-lavet, R. Fonteneau, and D. Ernst, "Deep Reinforcement Learning Solutions for Energy Microgrids Management," *Eur. Work. Reinf. Learn. (EWRL 2016)*, no. 2015, pp. 1–7, 2016, [Online]. Available: https://orbi.uliege.be/handle/2268/203831